JOURNAL OF AIRCRAFT
Vol. 34, No. 6, November–December 1997

Maneuvering Flight Performance Using the Linearized Propeller Polar

John T. Lowry*
Flight Physics, Billings, Montana 59104-0919

Fixed-pitch, propeller-driven, quasi-steady-state wings–level aircraft performance calculations are made simply and realistically by employing the linearized propeller polar formulation. This analysis extends that earlier treatment to banked turns and steady maneuvering. Building on the wings–level theory, it is useful to consider an absolute banked ceiling, the highest altitude at which the airplane can maintain level flight when banked through a particular angle. Because the linearized propeller polar (or bootstrap approach) is composed of such simple formulas, it is easy to construct a steady maneuvering diagram, giving the pilot immediate visualization of the relations among airspeed, bank angle, load factor limit, banked stall speed, rate of climb or descent, and either turning radius or rate. A precise prescription for constructing such a steady maneuvering diagram is given. For level turns, expressions for minimum turn radius and maximum turning rate are also given. It is found that these expressions for optimum turns are operational and not overshadowed by banked stall speed limits. These banked bootstrap-turning results are at considerable variance from the standard theory that assumes constant propeller efficiency and constant power. It is concluded that this extended linearized propeller polar analysis is easy to calculate and visualize and that it should be used more extensively in both pilot training and aircraft operations.

Nomenclature

A = wing aspect ratio, span^2/area
b = linearized propeller polar intercept
C = altitude engine power dropoff parameter
C_{D0} = parasite drag coefficient
$C_{L_{max}}$ = maximum lift coefficient
C_P = propeller power coefficient
C_T = propeller thrust coefficient
D = drag
d = propeller diameter
E = composite bootstrap parameter
e = Oswald airplane efficiency factor
F = composite bootstrap parameter
G = composite bootstrap parameter
H = composite bootstrap parameter
$\dot{h}$ = rate of climb
J = propeller advance ratio
K = composite bootstrap parameter
L = lift
M = engine torque
m = linearized propeller polar slope
n = propeller rps; load factor
P = power
Q = composite bootstrap parameter
R = aircraft turn radius; composite bootstrap parameter
S = reference wing area
T = thrust
U = composite bootstrap parameter
V = airspeed
W = gross aircraft weight
γ = flight-path angle
ΔS = stall speed buffer speed
δ_f = flaps deflection angle
η = propeller efficiency
ρ = atmospheric density
σ = relative atmospheric density
Φ = engine torque/power dropoff factor
ϕ = aircraft bank angle
ω = aircraft turning rate

Subscripts
AC = absolute ceiling
a = available
B = base case, mean sea level, maximum gross weight
bg = best glide
i = induced
max = maximum for level flight
md = minimum descent rate
min = minimum for level flight
n lim = load factor limit
p = parasite
r = required
S = stall
x = best climb angle
xs = excess
y = best climb rate
0 = standard value

Introduction

MANEUVERING flight performance has traditionally been given fairly short shrift in propeller aircraft performance textbooks and monographs[1–4] for two sets of reasons. First, there are complications because of three very real limitations superimposed on the elementary centripetal force picture: 1) structural, the load factor g limit; 2) aerodynamic, the raised stall speed while banking; and 3) raised power or thrust requirements under the increased induced drag. Second, there are descriptive and mathematical difficulties. The turning performance problem is essentially multivariable. Because the pilot has control (within broad limits) over both V and ϕ, many different combinations of those lead to the same R or ω. The selection of optimum inputs must be sufficiently supported. In addition, some of the standard governing piston–propeller equations, even though based on oversimplified physical pictures of maneuvering, are nontrivial quartics that lead to dif-

Received Jan. 16, 1997; revision received June 13, 1997; accepted for publication June 13, 1997.

*Owner, 724 Alderson Avenue, P.O. Box 20919.

ficult analytic solutions. Two such oversimplifications are 1) restriction to level turns, with thrust and drag approximately equal, and 2) assumption of constant propeller efficiency or of constant engine power, unwarranted at these relatively low maneuvering speeds.

The performance formulation using a linearized propeller polar[5–7] has much to offer toward clarifying those muddy waters:

$$C_T/J^2 = mC_P/J^2 + b \tag{1}$$

The theory is also known by the shorter term, bootstrap approach, because in it one flies the airplane briefly, at one weight and altitude, to gather the parameters that describe the airplane's steady-state performance extensively at any weight or altitude.

The bootstrap approach is limited in both application and audience. Because this approach only describes the main, full-throttle, and gliding performance of rigid subsonic fixed-pitch, propeller-driven reciprocating-engine-powered aircraft with quadratic drag polars during quasi-steady-state coordinated maneuvers, it cannot take the place of the whole panoply of data collection and computer hardware and software or of the more exhaustive (including partial throttle) performance flight tests needed in the safe design and efficient operation of modern high-performance aircraft. The unaugmented bootstrap approach, for instance, has nothing to say about aircraft stall or spin characteristics, landing, or takeoff performance, or a whole host of accelerated maneuvers that might be examined by a conscientious manufacturer. The actual propeller polar, C_T/J^2 as a function of C_P/J^2, is never perfectly linear, but in practical cases it is fairly close; goodness-of-fit parameter $R^2 \doteq 0.96$ within typical applicable flight regimes. And while the bootstrap assumption that throttle position completely dictates engine torque (at given altitude) is not strictly correct, typical propeller/powerplant combinations show less than 5% variation in torque while the engine speed changes by as much as 700 rpm. The bootstrap approach is not an unassailable theory, but we believe it is a respectable one.

Extensions to other types of the bootstrap approach are possible and have been constructed. Constant-speed propeller aircraft can be brought into the fold by use of the (unpublished) General Aviation General Propeller Chart. That is, essentially, a recasting using general aviation propeller data of Boeing's venerable General Propeller Chart of World War II. Turbojet aircraft, if one does not look closely at the details, are in some respects simpler than propeller-driven ones. Treating turbojet maximum thrust as approximately constant with airspeed (ignoring ram and secondary effects), with that thrust depending on σ raised to some fractional power, gives a start in that direction.

The virtue of the bootstrap approach is that it gives student pilots, college aviation and engineering students, and aircraft designers, manufacturers, or modifiers a simple low-cost method of fairly accurately predicting the performance of general aviation propeller airplanes. Though experimental validation is presently not extensive (the method is currently being used by only a handful of small aircraft manufacturers and modifiers), the approach has so far proved surprisingly accurate and robust. Performance flight tests and calculations using the bootstrap approach take less than 5% of the time needed by a standard general aviation procedure. Wider use of the bootstrap approach could translate into quicker design cycles and higher profits for a beleaguered small aircraft industry.

Here, we extend the ordinary wings–level bootstrap approach to include steady coordinated turns. We find that this maneuvering version leads to simple heuristics and realistic and tractable equations. After introducing the main bootstrap parameters and their composite cousins, along with formulas for six important V speeds and other performance items, we display and derive a steady maneuvering chart. It was pointed out that our chart is very similar to the doghouse chart[8] long used to depict the turning performance of high-performance aircraft. (A minor difference is that the doghouse chart does not include explicit aircraft bank angles.) Our chart, in airspeed–bank-angle space, makes for easy visualization of operational tradeoffs and limitations and allows the convenient selection of safe and optimized operating procedures. An absolute banked ceiling, the greatest density altitude at which the airplane can fly level when banked through a specific angle, will be a useful ancillary concept. In contrast to the ordinary wings–level absolute ceiling, this ceiling is physically attainable; it is also easily calculated and surprisingly intuitive. Finally, we calculate, for level turns, expressions for minimum turning radius and maximum turning rate, and contrast our results with those of the standard theory.

Wings–Level Bootstrap Approach

Computing quasi-steady-state aircraft performance using the wings–level fixed-pitch normally aspirated version of the bootstrap approach requires the nine aircraft parameters exemplified, for a Cessna 172, in Table 1. Only C_{D0} and e depend on flap/gear configuration. In concrete application, one also has values for the two variables W and σ (or its surrogate h_p).

The proportional mechanical power loss independent of altitude C (which can almost always be taken as 0.12), governs full-throttle torque at altitude through the power dropoff factor Φ:

$$M(\sigma) = \Phi(\sigma) \times M_B \tag{2}$$

The time-honored form[9] for this dropoff factor is

$$\Phi(\sigma) = (\sigma - C)/(1 - C) \tag{3}$$

Instead of using rated MSL torque directly, it can be used through the more common MSL full-throttle power and engine rotation speed. The relation is

$$M_B = P_B/2\pi n_B \tag{4}$$

Practical work is sped up by using composite bootstrap parameters in forms that either do or do not incorporate explicit weight and altitude dependencies. The four required first-line composites are

$$E = \Phi(\sigma)E_B, \quad \text{with} \quad E_B = mP_B/n_B d \tag{5}$$

$$F = \sigma F_B, \quad \text{with} \quad F_B = \rho_0 d^2 b \tag{6}$$

$$G = \sigma G_B, \quad \text{with} \quad G_B = \tfrac{1}{2}\rho_0 S C_{D0} \tag{7}$$

$$H = \left(\frac{W}{W_B}\right)^2 \frac{1}{\sigma} H_B, \quad \text{with} \quad H_B = \frac{2W_B^2}{\rho_0 S\pi eA} \tag{8}$$

Table 1 Sample bootstrap parameters[a]

Bootstrap data plate item	Value	Aircraft subsystem
S, ft^2	174	Airframe
A	7.38	Airframe
Rated MSL torque M_B, ft-lbf	311.2	Engine
C	0.12	Engine
d, ft	6.25	Propeller
C_{D0}	0.037	Airframe
e	0.72	Airframe
m	1.70	Propeller
b	−0.0564	Propeller

[a]Cessna 172.

It is often convenient to use second-level composite bootstrap parameters:

$$K = \sigma K_B, \quad \text{with} \quad K_B = F_B - G_B \tag{9}$$

$$Q = \frac{\Phi(\sigma)}{\sigma} Q_B, \quad \text{with} \quad Q_B = E_B/K_B \tag{10}$$

$$R = \left(\frac{W}{W_B}\right)^2 \frac{1}{\sigma^2} R_B, \quad \text{with} \quad R_B = \frac{H_B}{K_B} \tag{11}$$

$$U = \left(\frac{W}{W_B}\right)^2 \frac{1}{\sigma^2} U_B, \quad \text{with} \quad U_B = \frac{H_B}{G_B} \tag{12}$$

Standard weight W_B is usually taken to be the airplane's maximum gross weight. Bootstrap formulas for the six V speeds, as true airspeeds in ft/s, are

$$V_{\max/\min} = \sqrt{\frac{-E \mp \sqrt{E^2 + 4KH}}{2K}} = \sqrt{-\frac{Q}{2} \pm \sqrt{\frac{Q^2}{4} + R}} \tag{13}$$

$$V_y = \sqrt{\frac{-E - \sqrt{E^2 - 12KH}}{6K}} = \sqrt{-\frac{Q}{6} + \sqrt{\frac{Q^2}{36} - \frac{R}{3}}} \tag{14}$$

$$V_x = \left(\frac{-H}{K}\right)^{1/4} = (-R)^{1/4} \tag{15}$$

$$V_{\text{bg}} = \left(\frac{H}{G}\right)^{1/4} = U^{1/4} \tag{16}$$

$$V_{\text{md}} = \left(\frac{H}{3G}\right)^{1/4} = \left(\frac{U}{3}\right)^{1/4} \doteq 0.7598 V_{\text{bg}} \tag{17}$$

These six V speed results[5] come directly from the following performance quantities:

$$P_a \equiv TV = EV + FV^3 \tag{18}$$

$$P_r \equiv DV = GV^3 + H/V \tag{19}$$

$$P_{\text{xs}} \equiv P_a - P_r = EV + KV^3 - H/V \tag{20}$$

$$T(V) = E + FV^2 \tag{21}$$

$$D(V) = D_p(V) + D_i(V) = GV^2 + H/V^2 \tag{22}$$

$$T_{\text{xs}} \equiv T - D = E + KV^2 - H/V^2 \tag{23}$$

In addition, it's useful to have formulas for

$$\text{ROC}(V) = \dot{h}(V) = \frac{P_{\text{xs}}(V)}{W} = \frac{EV + KV^3 - H/V}{W} \tag{24}$$

$$\gamma(V) = \sin^{-1}\frac{T_{\text{xs}}(V)}{W} = \sin^{-1}\left[\frac{E + KV^2 - H/V^2}{W}\right] \tag{25}$$

where ROC = rate of climb. The wings–level composite parameters are evaluated at three different altitudes in Table 2. Bootstrap absolute ceiling results will be given in later in this paper.

Extension of Bootstrap Approach to Maneuvering Flight

In wings–level, constant-altitude unaccelerated flight, to our approximation (no off-axis thrust component), L is equal to W. When the pilot wants to turn the airplane, he or she banks to some angle ϕ, tilting the lift vector toward the desired direction. To maintain altitude, the pilot also applies sufficient backstick, enlarging the vertical component of lift, to balance weight. Since increased lift means increased induced drag, the pilot must also add power if airspeed is to be held constant.

This additional induced drag while turning leads to the only modification of the wings–level bootstrap approach required to encompass quasi-steady-state maneuvering flight:

$$H \equiv H(0) \rightarrow H(\phi) \equiv H(0)/\cos^2\phi \tag{26}$$

(The parenthesized zero denotes a value for unbanked, wings–level, flight.) For most (not all) intents and purposes, banking to angle ϕ is tantamount to increasing gross weight from W to $W/\cos\phi$. Several banked V speeds transform precisely, as does the stall speed:

$$V_{S/\text{xbg/md}}(\phi) = \frac{V_{S/\text{xbg/md}}(0)}{\sqrt{\cos\phi}} \tag{27}$$

where the wings–level stall speed is given by

$$V_S(0) = \sqrt{\frac{2W\cos\gamma}{\rho S C_{L_{\max}}}} \doteq \sqrt{\frac{2W}{\rho S C_{L_{\max}}}} \tag{28}$$

For our sample Cessna, with flaps up, $C_{L_{\max}} = 1.54$. $V_x(0)$, $V_{\text{bg}}(0)$, and $V_{\text{md}}(0)$ are given by Eqs. (15–17) in the previous section. Figure 1 shows the effect, on speeds for best angle and rate of climb, of banking at two sample altitudes.

Speeds for the best rate of climb and for the minimum or maximum level flight are somewhat more complicated. In the

Table 2 Sample composite bootstrap parameters at three altitudes

Variable or composite	Case 1, MSL	Case 2, 6000 ft	Case 3, 12,000 ft
W	2400 lbf = W_B	2400 lbf = W_B	2400 lbf = W_B
σ	1.0000	0.8359	0.6932
$\Phi(\sigma)$	1.0000	0.8135	0.6513
E	531.911 = E_B	432.697	346.451
F	−0.0052368 = F_B	−0.0043772	−0.0036300
G	0.0076516 = G_B	0.0063956	0.0053039
H	1,668,535 = H_B	1,996,192	2,407,100
K	−0.0128884 = K_B	−0.0107729	−0.0089339
Q	−41,270.6 = Q_B	−40,165.4	−38,779.5
R	−129,460,301 = R_B	−185,297,929	−269,435,170
U	218,064,595 = U_B	312,118,214	453,840,065

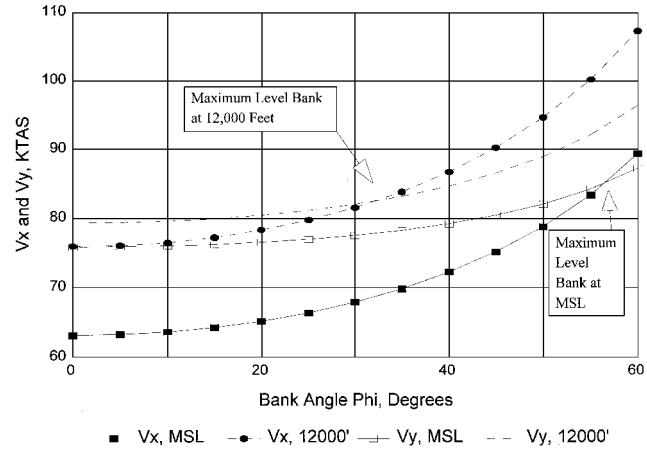

Fig. 1 Speeds V_y and V_x vs bank angle for two altitudes. Cessna 172, flaps up, 2400 lbf.

banked case, those three V speeds depend, instead of simply on $R = R(0)$ as in Eqs. (13) and (14), on

$$R(\phi) \equiv R(0)/\cos^2\phi \tag{29}$$

As is shown in Fig. 1, V_x is affected more by banking than V_y. That is because V_x depends on excess thrust, and induced drag drops off faster with airspeed than the induced power responsible for the speed dependence of V_y.

Figure 2 shows the dependence of minimum and maximum level flight and stall speeds on bank angle at two different altitudes.

Banked forms for rate and angle of climb are arrived at by substituting $H(\phi)$ for $H = H(0)$ in Eqs. (24) and (25). Figures 3 and 4 show the speed dependence of rate and angle of climb at MSL for four specific bank angles. Cutoffs on the left portions of those eight graphs are a result of impending stall speeds.

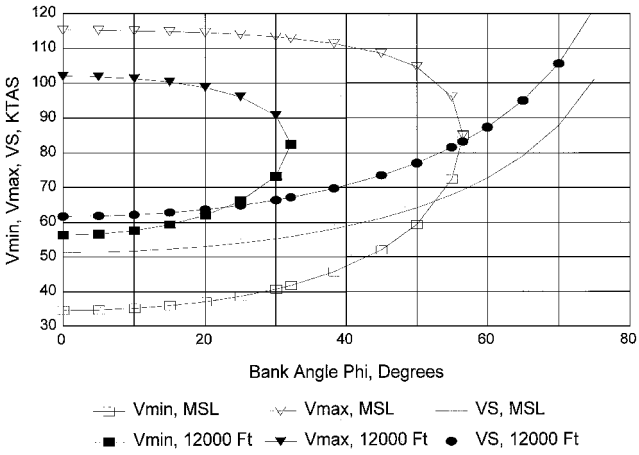

Fig. 2 Low and high speeds of level flight and stall speeds vs bank angle for two altitudes. Cessna 172, flaps up, 2400 lbf.

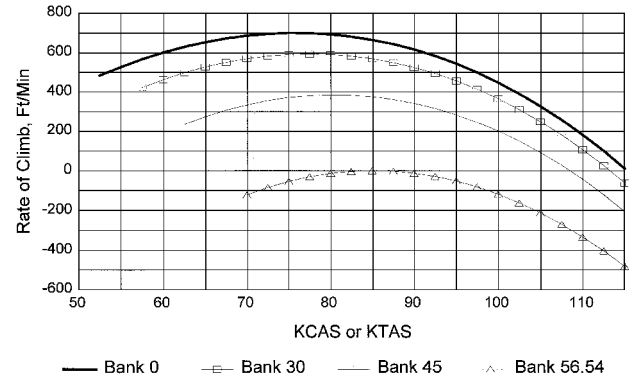

Fig. 3 Rate of climb vs airspeed for four bank angles. Cessna 172, MSL, flaps up, 2400 lbf.

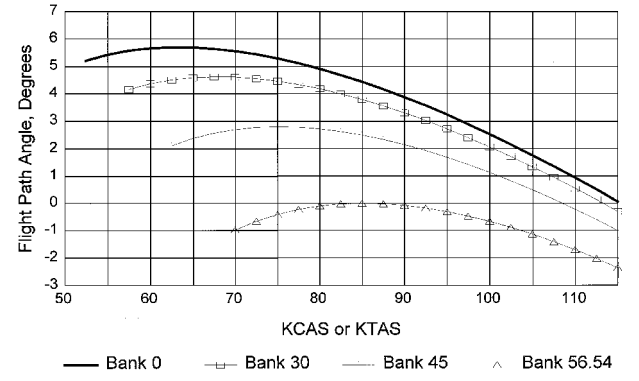

Fig. 4 Flight-path angle vs airspeed for four bank angles. Cessna 172, MSL, flaps up, 2400 lbf.

Banked or Unbanked Absolute Ceilings

An airplane's unbanked absolute ceiling, while perhaps a theoretical performance benchmark worthy of record, is not attainable. For the airplane at a given weight in given configuration there are two numbers involved: 1) the ceiling figure, a density altitude; and 2) the airspeed the aircraft requires to stay at that altitude (if dropped there by some higher-flying entity). The airplane's banked ceilings, however, are readily achieved; those are therefore a much more practical and interesting set of figures, one for each finite bank angle. The airplane's (banked or unbanked) absolute ceiling is characterized analytically by the graphs of P_a and P_r, using the possibly banked form of H, touching at one point. The expression of that osculation is that both P_{xs} and dP_{xs}/dV are zero. Using Eq. (20) to express that dual condition, one can use elementary methods to derive (somewhat circuitously) simple expressions for the required ceiling airspeed and altitude for given gross weight and bank angle:

$$V_{AC}(W, \phi) = \sqrt{2H(\phi)/E} \tag{30}$$

$$h_{\rho AC} = 145{,}457(1 - \sigma_{AC}^{0.234943}) \tag{31}$$

The ceiling relative air density is given in terms of the ceiling power dropoff factor

$$\sigma_{AC} = (1 - C)\Phi_{AC} + C \tag{32}$$

which, in turn, is given by

$$\Phi_{AC}(W, \phi) = \frac{2W}{W_B E_B \cos\phi}\sqrt{-K_B H_B(0)} \tag{33}$$

For our sample Cessna, wings level, and $W = 2400$ lbf, one may run through these last four formulas, in reverse order, to find $V_{AC} = 81.2$ knots true air speed (KTAS) = 63.2 knots calibrated air speed (KCAS), $\sigma_{AC} = 0.6052$, and $h_\rho = 16{,}187$ ft. Looking at Eq. (33) in a relative way gives the following useful relation:

$$\Phi_{AC}(W, \phi) = \frac{\Phi_{AC}(W, \phi = 0)}{\cos\phi} \tag{34}$$

Banking the airplane at some density altitude h_ρ is equivalent to dragging the ceiling down toward that altitude. Bank it enough, and the absolute banked ceiling descends onto the aircraft or even, temporarily, slides beneath it. If our sample Cessna banks 30 deg, for instance, its absolute ceiling is reduced from 16,187 to 12,587 ft. If the airplane is at a density altitude of 12,587 ft, it can bank more than 30 deg, but when it does so, its full-throttle best-climb angle and rate go negative and the aircraft descends to stabilize at a new and even lower banked ceiling. Each ceiling requires the specific airspeed given by Eq. (30). To maintain altitude, our wings-level Cessna at an absolute ceiling of 16,187 ft must fly at 63.2 KCAS; banked 30 deg at an absolute banked ceiling of 12,587 ft, it must fly at 67.9 KCAS. Both speeds are the pertinent speeds for the best angle of climb $V_x(W, \phi)$ which, in the bootstrap approach and expressed in calibrated (equivalent) terms, are independent of density altitude.

It is instructive to investigate the range of turning possibilities with this aircraft at its service ceiling ($\dot{h}_{max} = 100$ ft/min, at the appropriate V_y). By trial and error on h_ρ [using Eq. (24)], the maximum gross weight service ceiling is found to be 13,773 ft, with corresponding $V_y = 80.4$ KTAS. The maximum

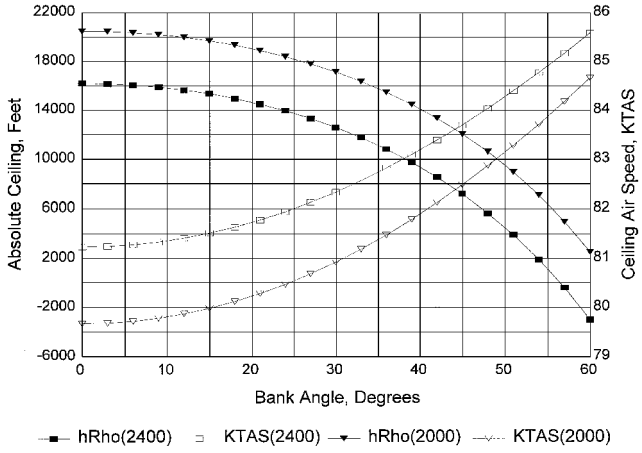

Fig. 5 Absolute ceiling and ceiling airspeed for two weights. Cessna 172, flaps up.

possible bank angle, before one starts down, is only 24.86 deg at 82.0 KTAS with turn radius R = 1285 ft. The minimum radius turn at this altitude, however (using techniques developed in the next section), is R = 1165 ft at 74.4 KTAS (about 8 kn above the 66.2-KTAS banked stall speed), banked 22.8 deg. This aircraft, if in the straitened circumstance of a narrowing canyon, is about to preclude the possibility of turning toward lowering terrain. Such circumstances cause some general aviation mountain flying accidents and provide a good reason for using steady maneuvering charts. Figure 5 shows banked absolute ceilings and ceiling air speeds for bank angles up to 60 deg for two aircraft weights.

Let us now consider W and h_ρ as given and inquire into the corresponding maximum permissible level-flight bank angle and ceiling speed. First, Eq. (31) is inverted to give

$$\sigma_{AC} = \left(1 - \frac{h_{\rho AC}}{145{,}457}\right)^{4.25635} \tag{35}$$

with Φ_{AC} then given by Eq. (2). Using Eq. (26) in the osculation condition then tells us the maximum bank angle for level flight at this altitude is

$$\phi_{AC} = \cos^{-1}[2\sqrt{-KH(0)/E}] \tag{36}$$

The corresponding ceiling airspeed is given by Eq. (30). These ceiling manipulations serve to show how simple bootstrap calculations are when one uses composite parameters and how intuitive the banked absolute ceiling concept soon becomes.

Steady Maneuvering Charts for Turn Radius and Turning Rate

A complete set of steady maneuvering charts (see Figs. 6–9 for examples) might consist of two dozen or more individual charts: perhaps for two gross weights, three density altitudes, two configurations, and the two outputs turn radius R and turning rate ω. While the number could be reduced by combining some of those, for clarity we won't combine them. Since maneuvering possibilities are enhanced by power, at least for low-performance aircraft, these will be full-throttle charts. Because the bootstrap approach is a variant of the venerable power-available/power-required analysis, the small flight-path angle is assumed. This means there are small errors (beyond any of the linearized propeller polar itself) in all the

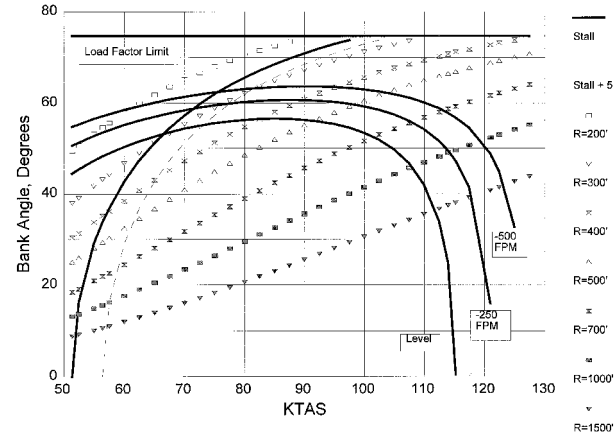

Fig. 6 Turn radius maneuvering chart for Cessna 172, MSL, lx flaps up, 2400 lbf.

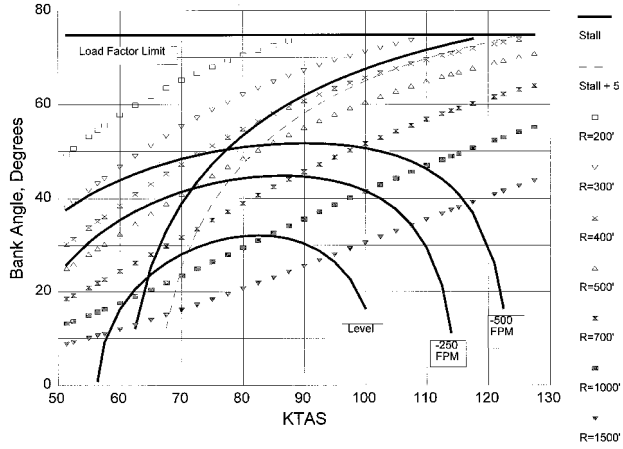

Fig. 7 Turn radius maneuvering chart for Cessna 172, 12000 ft, flaps up, 2400 lbf.

graphs making up the chart. But if one iterates [using Eq. (25) selectively for the flight-path angle], the errors will be found to be practically negligible except at extreme descent rates never used for steady turns.

The two outputs of interest are given by the following standard formulas:

$$R = V^2/g \tan \phi \tag{37}$$

$$\omega = V/R = g \tan \phi/V \tag{38}$$

It is clear from Eqs. (37) and (38) that desirable maneuvering characteristics, small R and large ω, both result from small values of V and large values of ϕ, but, as usual in aeronautical work, the devil is in the details. It is those details that the steady maneuvering charts are designed to elucidate. While these charts employ essentially the same independent variables, V and ϕ, as the more common V-n (sometimes, V-g) diagrams, their use is much different. The V-n diagram describes the flight envelope predominately in terms of quick control inputs, stalls, load factor limits, and the never-exceed speed. It includes negative-g (or inverted flight) possibilities. Quick noncontrol inputs, from gusts, are often overlaid on the V-n diagram. Our charts, on the contrary, consider only quasi-steady-state maneuvering (steady turns). Though the load factor limit is included, it is hardly ever a serious concern when using a steady maneuvering chart.

To use either of the steady maneuvering charts, one must provide answers to two questions: 1) how close to the stall is

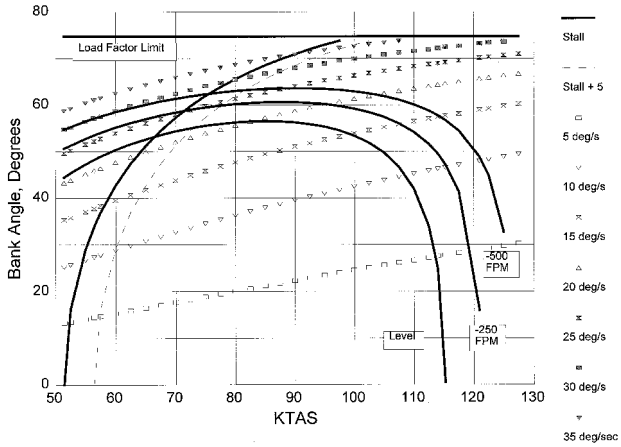

Fig. 8 Turn rate maneuvering chart for Cessna 172, MSL, flaps up, 2400 lbf.

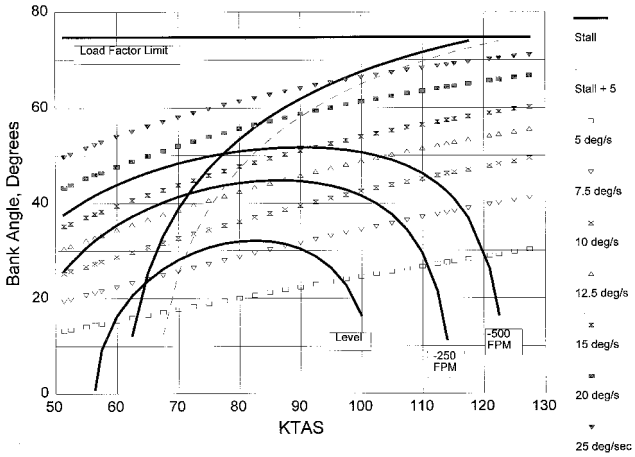

Fig. 9 Turn rate maneuvering chart for Cessna 172, 12000 ft, flaps up, 2400 lbf.

one willing to venture? and 2) how large a descent rate can one live with? If the answers are, respectively, 5 kn and 250 ft/min, then at MSL in our sample aircraft, Figs. 6 and 7 provide a turn radius of about 310 ft and a turning rate of about 25 deg/s, each at about 78 KTAS banked about 60 deg. If the airplane is up at 12,000 ft, however, Figs. 8 and 9 provide a turn radius of about 560 ft and a turning rate of about 14 deg/s, each at about 77 KTAS and banked about 44 deg.

If level turns were prescribed at 12,000 ft, then the pilot will get a minimum turn radius and a maximum turning rate at speeds greater than the banked stall speed. At higher altitudes, the curves of constant climb or descent rate have emerged from behind the limb of the banked stall curve. The standard maneuvering speed important in rough air, the speed at which the banked stall curve crosses the load factor limit, is too large here (119 KTAS) to be of significance for steady turns. High-performance aircraft may very well enter a turn with such excess speed (above the stall) that slowing down to enhance turn performance is a viable option. For low-performance aircraft, however, the inevitable slowing because of increased induced drag in the turn is about all they can afford.

To construct steady maneuvering charts for a specific airplane, one must have the nine bootstrap parameters for the desired flaps/gear configuration plus the appropriate positive g limit and $C_{L_{\max}}$. The procedure for getting the four harder-to-get parameters is adumbrated in Ref. 5 and given in full detail in Ref. 7. Next, a particular weight and density altitude is selected. The following five different kinds of curves can then be drawn.

Load Factor Limit

For the Cessna 172 normal category airplane, the flaps up-flight load factor limit is 3.8 g. That means

$$n \equiv \frac{L}{W} = \frac{W\cos\gamma}{W\cos\phi} \doteq \frac{1}{\cos\phi} \leq 3.8 \tag{39}$$

independent of V. The limiting bank is then

$$\phi_{n\text{lim}} = \cos^{-1}(1/3.8) = 74.74 \text{ deg} \tag{40}$$

Banked (and Padded) Stall Limit

Using Eqs. (27) and (28), allowing for the pad ΔS, and inverting

$$\phi_{S+\Delta S} = \cos^{-1}\left[\frac{2W}{\rho S C_{L_{\max}}(V_S(\phi) - \Delta S)^2}\right] \tag{41}$$

Curves of Constant Climb or Descent Rate

Using Eq. (26) in Eq. (24) and solving (using rate of climb h^* in ft/min)

$$\phi_{h^*} = \cos^{-1}\sqrt{\frac{H(0)}{V^2(E + KV^2) - Wh^*V/60}} \tag{42}$$

Curves of Constant Turn Radius R

Inverting Eq. (37)

$$\phi_R = \tan^{-1}(V^2/gR) \tag{43}$$

Curves of Constant Turning Rate ω

Inverting Eq. (38) (and using turning rate ω in deg/s)

$$\phi_\omega = \tan^{-1}(\pi V\omega/180g) \tag{44}$$

Because only the curves associated with stalling and with climb rate vary with density altitude, it doesn't take a great deal of effort to construct a full set of steady maneuver charts for a given airplane.

Level Maneuvering Flight Performance Results

As representative of the standard piston-propeller maneuvering theory, we take formulas derived by Hale,[4] also cited by Adamson,[2] for level (thrust equals drag) turns. Similar formulas are treated, somewhat more extensively and with fewer approximations, by Miele.[10] Those authors express the variables of interest, R and ω, in terms of the load factor n (standing in for ϕ) and V. To find optima, they differentiate those expressions with respect to V, set those derivatives equal to zero, and solve. With functions of two variables, one cannot in general be assured of successfully using that procedure to find relative minima or maxima of the full function. Kaplan[11] has a clear and simple counterexample. Because their resulting expressions are complicated, Hale[4] and Adamson[2] also make warranted discards of small terms. Results are to be taken as only indicative because their calculated airspeeds for optimal turns are considerably below the associated banked stall speeds.[2,4] That is also often the case when using our alternative calculation procedure but not always. At higher altitudes, the analytic relative optima may prevail. First consider turn radius $R(V, \phi)$, given by Eq. (37). In the bootstrap approach, because the low speed for level flight is concerned, we have Eq. (13) for $V(\phi)$ or, because $\gamma = 0$, we can solve that specialization of Eq. (25) for $\phi(V)$. Neither of the resulting expressions, in this level case, is particularly complex and neither requires approximation. Using both of those procedures, ordinary calculus gives

$$\phi_{\min R} = \tan^{-1}\sqrt{1 + [4H(0)/KQ^2]} \tag{45}$$

Table 3 Optimum level turns, standard, and bootstrap approaches

Value for optimum	Standard approach	Bootstrap approach
$V_{\min R}$	43.7 KTAS	69.8 KTAS
$\phi_{\min R}$	30.0 deg	28.0 deg
$R_{\min}$	292 ft	813 ft
$V_{\max\omega}$	65.5 KTAS	75.9 KTAS
$\phi_{\max\omega}$	45.0 deg	31.0 deg
$\omega_{\max}$	16.7 deg/s	8.6 deg/s

which shows, since the radicand is less than unity, that $\phi_{\min R}$ is always less than 45 deg, and

$$V_{\min R} = \sqrt{2H(0)/E} \tag{46}$$

The search for inputs giving a maximum turning rate also provides fairly simple results:

$$\phi_{\max\omega} = \tan^{-1}\sqrt{-2 - Q\sqrt{(-K)/H(0)}} \tag{47}$$

$$V_{\max\omega} = \left[\frac{-H(0)}{K}\right]^{1/4} \tag{48}$$

The subscripts min R and max ω must be interpreted in a provisional sense. To see whether the banked stall speed is higher, and therefore overriding, the appropriate steady maneuvering chart, or an ancillary calculation, must be consulted.

The corresponding approximations from Hale[4] are

$$\phi_{\min R} \doteq 30 \text{ deg} \tag{49}$$

independent of weight or altitude

$$V_{\min R} \doteq \frac{8W^2}{3 \times 550\eta\rho S\pi eA(\text{hp})} \tag{50}$$

and, for maximum turning rate

$$\phi_{\max\omega} \doteq 45 \text{ deg} \tag{51}$$

$$V_{\max\omega} \doteq \frac{4W^2}{550\eta\rho S\pi eA(\text{hp})} = \frac{3}{2} V_{\min R} \tag{52}$$

Table 3 gives a detailed comparison for our sample Cessna 172, flaps up, at 12,000 ft at W = 2400 lbf. Both standard approach optimum speeds are less than the actual banked stall speeds and are therefore not operationally feasible. For this relatively high-altitude case, the bootstrap approach results are greater than the actual banked stall speeds.

Conclusions

The linearized propeller polar or bootstrap approach is easily generalized to encompass maneuvering flight. It gives simple analytic results for the main variables of interest: banked (or unbanked) ceiling specifications, turn radius, turning rate, and specification of optimum level conditions for the latter two results. Steady maneuvering charts for a range of weight and altitude situations are fairly easily constructed. Those provide a graphic display of operational limitations and suggest optimum safe turning speeds and bank angles for any given situation. To promote safe operation, pilot training ground schools should demonstrate the use of steady maneuvering charts, and general aviation aircraft manufacturers should consider including such charts in the approved flight manuals for their aircraft. The linearized propeller polar is less restricted, in its sphere of application, than the current standard approach to maneuvering calculations. It also gives more realistic results at considerable variance from the standard approach.

References

[1]Hurt, H. H., *Aerodynamics for Naval Aviators*, U.S. Navy, 1965, pp. 176–182.

[2]Adamson, J. C., *Aircraft Performance*, U.S. Military Academy, 1991, Chaps. 27, 30.

[3]Perkins, C. D., and Hage, R. E., *Airplane Performance Stability and Control*, Wiley, New York, 1949, pp. 201–203.

[4]Hale, F. J., *Aircraft Performance, Selection, and Design*, Wiley, New York, 1984, pp. 151–160.

[5]Lowry, J. T., "Analytic V Speeds from Linearized Propeller Polar," *Journal of Aircraft*, Vol. 33, No. 1, 1996, pp. 233–235.

[6]Lowry, J. T., "The Bootstrap Approach to Predicting Airplane Flight Performance," *Journal of Aviation/Aerospace Education and Research*, Vol. 6, No. 1, 1995, pp. 25–33.

[7]Lowry, J. T., *Computing Airplane Performance with the Bootstrap Approach: A Field Guide*, M Press, Billings, MT, 1995.

[8]Ward, D. T., *Introduction to Flight Test Engineering*, Elsevier, New York, 1993, Chap. 3.

[9]Gagg, R. F., and Farrar, E. V., "Altitude Performance of Aircraft Engines Equipped with Gear-Driven Superchargers," *SAE Transactions*, Vol. 29, No. 3, 1934, pp. 217–223.

[10]Miele, A., *Flight Mechanics-1: Theory of Flight Paths*, Addison–Wesley, Reading, MA, 1962, pp. 149–189.

[11]Kaplan, W., *Advanced Calculus*, Addison–Wesley, Reading, MA, 1952, pp. 122–124.